NISTIR 6197

Report on the First-Generation NIST Convective Heat Flux Calibration Facility

David G. Holmberg
Carole A. Womeldorf

Fire Science Division
Building and Fire Research Laboratory
Gaithersburg, MD 20899

United States Department of Commerce
Technology Administration
National Institute of Standards and Technology

NISTIR 6197

Report on the First-Generation NIST Convective Heat Flux Calibration Facility

Prepared for
U.S. Department of Commerce
National Institute of Standards and Technology
Gaithersburg, MD 20899

By
David G. Holmberg
Carole A. Womeldorf
Fire Science Division
Building and Fire Research Laboratory
National Institute of Standards and Technology

December, 1998

U.S. DEPARTMENT OF COMMERCE
William M. Daley, Secretary

TECHNOLOGY ADMINISTRATION
Gary Bachula, Acting Under Secretary for Technology

NATIONAL INSTITUTE OF STANDARDS
Raymond G. Kammer, Director

ABSTRACT

The National Institute of Standards and Technology has developed a convective heat flux calibration facility to allow evaluation of heat flux sensors. This facility is a small wind tunnel that produces a two-dimensional laminar boundary layer across a heated iso-thermal copper plate. This facility has been developed to allow convection calibration of heat flux sensors to complement heat flux sensor calibrations presently conducted using standard radiation methods, recognizing that many sensors are used in mixed radiation and convection environments. By extending calibration capabilities to include a primarily convective environment, direct comparisons of sensors in controlled convective and radiative environments are possible.

This report describes the first-generation heated plate design, analysis, and performance. The reference heat flux on the plate is found from the electrical power input to a guarded region of the plate to the side of the sensor in the spanwise uniform flow. Tests have demonstrated a repeatability on the reference heat flux of ± 1.5 %. A detailed uncertainty analysis of the reference heat flux value is presented showing lateral conduction to surrounding regions of the plate to be the greatest source of uncertainty with plate surface emissivity the only other significant source. The calculated relative expanded uncertainty (95 % level of confidence) on the measured reference heat flux value is ± 4.6 %. The average reference heat flux from these tests agrees with numerical predictions within 2 %.

An independent measure of the reference heat flux has been employed to demonstrate absolute accuracy of the facility. Tests using a conduction calibration agree within 1 % with the plate reference. This 1 % difference gives increased confidence in the absolute accuracy of the convection facility and compares favorably with the calculated 4.6 % uncertainty.

Development of a second generation heated plate continues with the goal of reducing uncertainty on the reference heat flux and improving the comparability of the heat flux at the sensor location to the reference heat flux by reducing radiation from the sensor and improving the sensor mounting arrangement.

INTRODUCTION

Heat flux sensors are typically calibrated in a known radiation flux, but applied in a combined radiation and convection environment. The heat transfer community has recognized that this dichotomy contributes to relative measurement uncertainties no better than ± 10 % [1]. A collective realization of the absence of standards for calibration and the lack of understanding of the issues involved in heat transfer measurement led the American Society of Mechanical Engineers (ASME) Heat Transfer Division to form a committee which organized a workshop in January 1995 of the heat transfer community at the National Institute of Standards and Technology (NIST). The purpose of this workshop was to discuss calibration and measurement issues and to delineate the current NIST calibration project. A full report of this workshop is given in reference [2], while a good summary is presented in [1].

The primary goal of the NIST project is to develop three heat flux calibration facilities as standards for calibration to a desired relative uncertainty of ± 2 %. The first facility is the low-speed convection wind tunnel discussed herein which allows calibration in a well defined laminar shear flow with flux levels up to 6 kW/m^2. The second facility is a higher flux conduction facility [3], and the third, an upgraded radiation facility [4]. For the first time, these facilities will allow a sensor to be calibrated at NIST in each of the three heat flux modes independently.

BACKGROUND

Heat flux is the movement of thermal energy through a surface, with units of power per area. This flow is controlled by material properties as well as by surface boundary conditions: fluid motion and properties, and radiation characteristics. It is fundamentally difficult to measure this energy flow without disturbing it—each sensor has structure with varying material properties that can disturb the flow of energy through the sensor, and surface properties that differ from the surrounding surface. Accurate measurement of heat flux requires understanding the errors produced by any given sensor which may vary depending on the nature of the incident energy. Heat flux calibration and measurement are not simple because the output from the sensor depends not only on the heat load, but on its thermal boundary conditions.

The three modes of heat transfer are conduction, convection, and radiation. Heat transfer from a sensor attached to a heated surface is generally by conduction to the sensor surface and from the surface by convection to the air and radiation to the surroundings. Conduction through the sensor will be distorted by the sensor structure. If the sensor structure includes lower thermal conductivity elements (such as adhesive or resistance layers) these can significantly alter the surface temperature profile relative to the surrounding surface and thus change the local heat flux. Convection acts at the interface of the sensor and fluid above and will be disrupted if there is any change in surface roughness or discontinuity of the surface profile. Radiation is defined in terms of wavelength spectrum, intensity, and angular distribution. Any given sensor absorbs, reflects, and transmits according to its own surface properties which

may not match those of the surrounding surface. Therefore, the structure and surface properties of the sensor can significantly change the flux through the sensor relative to the desired undisturbed flux through the surrounding surface.

The need for convection calibration can be seen when considering these effects. A radiation calibration is relatively insensitive to sensor temperature due to the large source to sensor temperature difference and does not include convective flow disturbances due to the presence of the sensor. The driving potential in convection is a much smaller flow to sensor temperature difference that can be significantly altered by sensor surface temperature mismatch to the surrounding substrate.

MEASUREMENT OF HEAT FLUX AND THE NIST CONVECTION FACILITY

Measurement of heat flux is performed using a variety of methods which can be classified in three categories [5]: (1) a temperature difference measured across a material of known thickness and thermal conductivity, (2) a temperature difference measured over time with a known thermal capacitance, and (3) a direct measure of the energy transfer made at steady conditions. References [5-7] review these methods and some of their different applications.

NIST's convective heat flux facility uses a steady state electrical heater output (category three above) as a reference. Because the facility operates at steady state, it is not configured to provide a reference heat flux value for transient (category two) temperature measurements. Instead, the facility is designed to test category one sensors that directly measure heat flux.

Users of these gages can be roughly classified into two groups. The first uses sensors in hot flow, at high flux levels and high air temperatures, represented by the external aerodynamic application, a fire environment, or measurements within a combustion engine. Radiation is often a large component of the total flux. The measurement surface is typically metal with inserted category one plug-type sensors which may or may not be cooled. However, category two temperature measurements are also common, allowing mathematical conversion to heat flux for short duration tests.

The second group uses sensors in cool flow, lower flux, surface cooling applications, such as for electronic cooling or process control. This group also includes those measuring heat flux at the lowest flux levels through insulation. Radiation, free and forced convection, and conduction can all be significant modes of heat transfer. Category one methods predominate, with a wide variety of sensors including inserted plug-type sensors as well as larger flat thermopile sensors commonly used for low flux levels when spatial resolution is not needed.

Development of the NIST convective heat flux facility has been driven by users of the first group and their need for improved accuracy in strongly convective and radiative environments. The present NIST facility is best suited for mounting the insert plug-type sensors, and can also handle some of the smaller flat sensors. The facility operates at lower fluxes than optimum for the first group and the flux is from surface to flow rather than flow to surface. However, these limitations were accepted in order to maximize accuracy for this primary facility. It is well suited to the flux magnitudes and flux direction required by the second user group. The NIST facility will be used to research heat transfer issues of benefit to both user groups, such as the sensitivity of different sensor types to convection versus radiation, the effects of sensor mounting, and the influence of surface coatings.

FACILITY DESIGN

The convection facility is a small open-loop wind tunnel with flow conditioning designed to produce a repeatable two-dimensional laminar flow across a heat flux sensor embedded in a heated isothermal plate. The maximum heat flux with the present configuration is approximately 5 kW/m^2. Measurements from the sensor are calibrated against the power required to heat a guarded reference section located alongside the sensor in the plate. A schematic of the plate and reference heat flux with respect to the sensor is shown in Fig. 1. Following are details of the wind tunnel construction, test section components, and instrumentation.

Flow Conditioning

The convection facility is depicted in Figure 2. Elements upstream of the test section constitute the flow generation and conditioning portion of the facility. Flow is generated by a 94.4 L/s blower, driven by a 0.746 kW AC motor equipped with a variable-frequency drive which permits speeds to be set in 0.1 Hz increments with 60 Hz full scale. The flow is then passed through the following conditioning elements which, unless described otherwise, are made of 12.7 mm-thick high-pressure phenolic laminate:

Muffler – a 1.2 m x 1 m x 0.5 m (inside dimensions) box of 19 mm plywood, lined with open-cell "egg crate" foam, and sized to damp out blower fan acoustic noise. Inlet and outlet connections are through nominal 102 mm ID rigid plastic pipe fitted with rubber vibration isolators.

Round-to-square transition – a sheet metal duct with a 102 mm round inlet and a 102 mm square outlet covered with a course mesh screen.

First diffuser – an 899 mm long unit which expands flow cross section to 275 mm x 254 mm. An aluminum splitter plate on the vertical centerline and another on the horizontal centerline divide the diffuser into four equal channels.

Heat exchanger – three Al liquid-to-air, tube-fin heat exchangers.

Second diffuser – a 216 mm-long unit which expands the flow cross section to 300 mm x 300 mm, with the same splitter-plate arrangement as in the first diffuser.

Honeycomb – a 207 mm section of aluminum honeycomb, with 6 mm hexagonal cells.

Screen section – a combination of three stainless steel square mesh screen assemblies, with screens of progressively smaller mesh: 0.85 mm, 0.65 mm, and 0.51 mm wire spacing respectively.

Settling section – a 338 mm-long duct.

Contracting nozzle

The contraction is a 164 mm-long, aluminum, two-dimensional nozzle. It reduces the flow cross section from 300 mm x 300 mm to 10 mm x 300 mm. The curved boundary was prescribed based on the approach of reference [8] and is defined by the equations

$$y[\text{mm}] = \pm \begin{cases} 5.+0.9667\left(150.-.00005487x^3\right); & 0 \le x \le 135\text{mm} \\ 5.+0.004296(150.-x)^3; & 135\text{mm} \le x \le 150\text{mm} \end{cases}$$

where x is in the streamwise direction (Figure 2). The 30:1 contraction ratio was chosen to minimize inlet turbulence intensity and provide a "top-hat" velocity profile. The nozzle geometry was analyzed using a finite-element code that predicted exit velocity profiles for given inlet velocity profiles. Results showed that there was no significant difference in the effect of a uniform inlet velocity profile vs. a parabolic profile on the outlet velocity profile indicating that the outlet profile is independent of the inlet profile.

Hot-wire anemometry was used to measure the velocity profile exiting the nozzle, test section removed, shown in Fig. 3. This profile was measured with the air flow at the highest Reynolds number attainable (Re_h = 20,000, height h = 10 mm). The entire boundary layer is only 0.5 mm thick, with a slight overshoot at the wall due to the just completed strong contraction, U_{max}/ U_{center} = 1.03. Corrections for near wall effects were done according to the method given by Wills [9], with corrections of less than 1% outside the boundary layer, 2% at 0.4 mm, 6% at 0.25 mm, and 30% at 0.1 mm (a 30% decrease from the measured velocity). Absolute accuracy in placing the hot-wire was accomplished by traversing the wire to the wall until it touched. Calibration was performed in a laminar jet calibrator apparatus. Multiple probes, calibrations, and traverses have demonstrated uncertainties in the measured U_{center} velocity of ± 1% (primarily due to probe differences, with individual probes giving repeatability of ± 0.2 % estimated standard deviation), and ± 0.03 mm in spatial location relative to the wall.

The turbulence intensity (defined here as the rms fluctuating component of velocity divided by the mean center velocity) leaving the nozzle is approximately 0.2 % outside of the boundary layer and less than 1% everywhere, with the measured increase in the boundary layer perhaps due to probe interference effects. Hot-wire measurements have shown that the flow is spanwise uniform. Smoke flow visualization has shown the presence of corner vortex pairs disturbing the flow near the test section sides. These vortices appear to influence the boundary layer out to about 40 mm from the sides or 13 % of the passage flow on each side. This disturbed region does not affect the reference heat flux and is contained within the outer guarded side areas of the plate.

Heated plate

The design of the test section includes a heated, isothermal, copper plate beneath a laminar shear flow of room temperature air. A bottom view of the first-generation plate is shown in Figure 4. The grooves divide the plate into thermally semi-isolated regions, for a total of 6 regions (labeled A-F) heated independently by six DC power supplies. The paired regions (A, B, and C) are joined in series. By independently heating the six regions, temperature

variation can be controlled and conductive perimeter losses can be compensated. Polyimide/metal foil resistance heaters (0.2 mm thick) are attached with a pressure sensitive adhesive layer to the bottom of each region. Below the heaters is a layer of insulation and beneath this a guard heater to null bottom conductive losses. Additional insulation and a support plate are beneath this, with the entire sandwich held in place by a clamp pressing the plate upward against the precision-located sidewalls to reference the plate leading edge to the nozzle exit.

The heat flux sensor mounts in a copper cylinder (sensor housing, Fig. 4) that seats against the lip seen in the center hole of the plate in Fig. 4. This allows the sensor surface to be set flush with the upper surface of the plate at a known distance from the inlet of the test section.

Reference region

The reference value for the desired true (undisturbed) heat flux at the sensor location is determined from the power input to the region of the plate labeled REF in Fig. 4. Power is found by measuring voltage across the REF region heater along with the voltage drop across a precision resistor to measure heater current. Power to surrounding regions and the lower guard heater are adjusted to null conduction into or out of the reference region so that all the power input to the REF region exits only from the upper surface.

The plate surface temperature is monitored with 32 fine gage (36 awg) type-T (Copper-Constantan) thermocouples. Careful ice-point calibration of these thermocouples has allowed uncertainties of 0.05 K for absolute temperature measurements. Two differential thermocouple pairs on each side of the REF region monitor the temperature difference across the bridge spanning the air gap. Tests have demonstrated 0.01 K accuracy for these differential measurements (0.01 K uncertainty at a 95 % level of confidence, based on statistical analysis of data samples). Power adjustments to surrounding regions allow the temperature difference across the gap to be nulled. The thermocouple, differential thermocouple, heat flux sensor, and power signals are collected with a PC-based data acquisition system. A feedback control algorithm automatically adjusts power to the heaters in order to minimize temperature differences and thereby null lateral conduction.

UNCERTAINTY ANALYSIS FOR THE HEATED PLATE

The reference heat flux value is based on knowing the energy transferred from the reference area to the air flow above and by radiation to the surroundings. The reference area must be guarded to prevent conductive heat transfer from the reference heater to and from surrounding regions in the plate. Conduction out the bottom must also be controlled and other losses accounted for. Uncertainties arise from system limitations on controlling parasitic conduction to surrounding regions within the plate, and knowledge of surface radiation properties. Relating the reference heat flux to the flux at the sensor introduces additional uncertainties. In this section, uncertainties of the reference heat flux value will be discussed, first looking at conduction uncertainties and then at the radiation uncertainties. Finally, an analysis is given for additional uncertainties in relating the heat flux from a test gage mounted in the hot plate to the reference value.

It will be shown that the primary uncertainty is due to lateral conduction to or from the reference area to surrounding regions. This uncertainty is absolute, controlled by the accuracy to which the temperature between regions can be measured as well as by thermal gradients present in the plate which create non-uniform plate temperatures within regions. This lateral conduction flux is independent of the convective flux to the flow. Therefore, the percentage of this lateral flux relative to the convective flux decreases with increasing plate to air temperature difference. Testing has been performed at temperature differences up to 100 K.

I. Reference Heat Flux Uncertainties

A. *Conduction within plate*

The reference area is 32.0 mm x 54.0 mm, plus a surrounding gap width of 3.2 mm. The reference heated area includes half the gap width, where the actual deviation from this is very small and discussed further in a later section. Therefore, the total heated area including half the gap width is 2.01×10^{-3} m^2. Uncertainty estimates will be made for a plate temperature to flow temperature difference ΔT_{flow} = 40 K. The convective energy transferred from the reference section to the flow, based on the convective numerical model described later is q_{conv} = 4.90 W, or q''_{conv} = 2440 W/m^2.

1. Lateral conduction analysis. Lateral conduction is affected by several parameters, shown in Fig. 5. The copper surface bridges the air gap separating the reference area from surrounding heated regions. Lateral conduction across this metal bridge increases with plate thermal conductivity and bridge thickness, but decreases with gap width.

The accuracy of the differential temperature measurement, 0.01 K stated earlier, is that between the two thermocouple beads. However, because of thermal gradients in the plate, this value is not necessarily the average difference across the bridge along the length of a reference area side. Taking the average of two differential thermocouples along each side helps to minimize this uncertainty. For this analysis, the uncertainty (estimated standard deviation based on system experience and modeling results) on the temperature difference across the gap will be taken as $\Delta T_{gap} = 0.025$ K.

The conduction across the bridge around the reference section is

$$q_{gap} = kPd\frac{\Delta T_{gap}}{w};$$

k = 400 W/mK; P is the perimeter, measured at the gap center (0.185 m); d is the bridge thickness (0.38 mm); and w is the gap width (3.2 mm). The amount of energy transferred across the gap if there is an undetected 0.025 K temperature difference between the reference area and all surrounding regions is $q_{gap} = 0.22$ W. This amount of heat transfer cannot be reduced with the present plate because it is derived from the physical system and the accuracy of temperature measurement. This is, however, a worst case, in that there are four independently heated regions bordering the reference area. A more realistic uncertainty on the lateral conduction would be the square root of the sum of the squares of the maximum error for each of the four sides, $q_{gap} = 0.11$ W. Taking this as the uncertainty due to uncontrollable conductive heat transfer to surrounding regions, the current design (at $\Delta T_{flow} = 40$ K) has a *lateral conduction uncertainty* (estimated standard deviation on lateral conduction) = $q_{gap}/q_{conv} = 2.2$ %.

In the air gap, lateral conduction and natural convection have been considered. Heat transfer by conduction through the air is less than 0.01 % of the reference convective flux. Natural convection can be judged with reference to classical correlations. Because the air gap is close to isothermal, the Rayleigh number turns out to be more than 2 orders of magnitude less than the critical value above which natural convection would occur. Thus, the air is stationary with insignificant conduction.

2. Reference section bottom losses. Thermocouples embedded at two different vertical locations in the foam beneath the reference heater allow monitoring the temperature gradient across the foam and nulling it by adjusting power to the guard heater. Based on experience, because temperature gradients in the foam are larger than in the plate, a temperature uncertainty across the insulation of 1 K is assumed. The total area of heat transfer is approximately equal to the reference area of $2\text{x}10^{-3}$ m^2. The compressed foam has a measured thermal conductivity of $k_{foam} = 0.030 \pm 10$ % W/mK and a thickness of h = 0.010 m. Therefore the uncertainty in the bottom conductive loss is $q_{cond,\ bottom} = k_{foam} \cdot A \cdot \Delta T/h = 0.006$ W. This amount of energy, transferred across the foam insulation assuming a 1 K temperature difference, results in a *bottom conduction uncertainty* of $q_{cond,\ bottom}/q_{conv} = 0.1$ %.

3. Wire conduction losses. Both thermocouple leads and power leads to the heaters are paths for conduction away from the heated plate. The thermocouple leads are Teflon coated 36 awg wire, while the heater wires are stranded copper. These leads exit the reference area below the heaters, cross the gap to the neighboring regions, and then are routed along the bottom of the plate and out through the insulation to room air. The wires remain in a nearly isothermal environment for at least 100 mm. Accordingly, their impact can be estimated in a manner similar to the upper gap bridge. Neglecting conduction along the insulation, 4 thermocouple wires, 8 differential thermocouple wires, and two heater wires (19 strands each) have a net cross section of 1.2 mm^2. Taking the conductivity of all the wires at $k_{Cu} = 400$ W/mK, and a conservative estimate of $\Delta T = 0.1$ K across the 0.32 mm gap, the q_{loss} will be $1.4\text{x}10^{-4}$ W, or less than 0.003% of q_{conv}.

4. Reference surface area. Knowing the heated surface area of the reference region is crucial to knowing the reference flux; several uncertainties are involved. First, how accurate is the machining so that we know the physical size of the reference region and gap width? Second, what percentage of the bridge is heated by the reference heater at the balanced condition? Third, how accurately is the heat flux known as a function of downstream distance along the plate in order to know the relationship between the sensor flux and the reference flux? The measured reference power is an average value over the heated area. This area itself depends on the streamwise heat flux distribution since the non-uniform heat flux profile across the upstream and downstream bridge areas will lead to a non-symmetrical temperature profile across the bridge.

The machining inaccuracy is likely very small with tolerances of 0.02 mm typical. With these small errors randomly distributed the effect on the calculated reference heat flux is negligible.

The second and third questions can be addressed both by numerical modeling (discussed below) and by

reference to theoretical isothermal flat plate heat transfer which varies as $x^{-1/2}$; x = distance from the plate leading edge. A simple 1-D analytical solution of the conduction and convection in the bridge, using this $x^{-1/2}$ profile, and a "balanced" condition defined such that the endpoints of the bridge are at the same temperature, gives the temperature distribution in the bridge. The point where the lateral heat flux within the bridge goes to zero (the minimum temperature point, T_{min}) is not at the center of the bridge, but displaced slightly upstream. With gap dimensions as given in Fig. 5, T_{min} in the bridge is shifted 0.33 % of the gap width from the center (a 0.01 mm shift) for the bridge on the upstream side of the reference region, and 0.12 % upstream on the downstream side of the reference region. These values then define the proper size of the area heated by the reference heater at the balanced condition with very small uncertainty. The proper spanwise dimension of the reference area extends to half the gap width assuming the heat flux is constant across the plate in the spanwise direction away from the sidewalls based on two-dimensionality of the flow.

The third question can also be addressed using an $x^{-1/2}$ streamwise heat transfer distribution. Integration of this profile across the reference area produces an average heat flux proportional to the measured reference heat flux. The flux at the sensor, taken as a point measurement, equals the flux at the center of the reference area. Based on this distribution, the ratio of the heat flux at the center point to the average is $q''_{sens}/ q''_{ref} = 0.969$. This agrees with the numerical solution to the conjugate conduction and convection heat transfer problem discussed below.

B. *Radiation from the plate*

The present plate emissivity is uncertain because *in-situ* measurements were not performed and the polished surface has light oxidation (in the second generation plate, a non-oxidizing surface will be used). An estimate of the current surface emissivity is $\varepsilon_{ref} = 0.10 \pm 0.05$. Taking the surroundings (test section top surface, nozzle, room walls, etc.) at room temperature, we can simplify the view factor to F = 1.0 and regard the surroundings as a hemispherical blackbody at room temperature (297 K). Then the radiation heat transfer from the reference area is 29.0 ± 14.5 W/m^2, given T_{ref} equal to 337 K. This flux is 1.2 % of the convective flux at T_{flow} = 40 K, with 0.6 % relative uncertainty, or an estimated standard deviation on the reference radiation component, due to emissivity uncertainty, of 0.6 %.

The combined standard uncertainty on the reference heat flux for the present heated plate design operating at ΔT_{flow} = 40 K, taken as the square root of the sum of the squares of the radiation, lateral, and bottom conduction uncertainties discussed above, is u_c = 2.3 %. Assuming that the measured reference heat flux values will follow a normal distribution, with a standard deviation of approximately 2.3 %, then the actual true heat flux, including convective and radiative components, will be q''_{ref} ± 4.6 %, where U = 4.6 % is the expanded uncertainty and a coverage factor of k = 2 has been applied so that the unknown true value lies within the interval of $U = k \cdot u_c$ with a level of confidence of approximately 95 %.

II. Sensor Heat Flux Uncertainties

A. *Conduction within sensor housing*

The present housing for cylindrical inserted 6.35 mm sensors is made of copper. The sensor has a sliding fit in the center hole and is held in place with a set screw and thermal grease to increase conduction to the sensor from the housing. The sensor housing itself is similarly mounted in the plate with a sliding fit and thermal grease. Housing and sensor rely on heating by conduction from the surrounding plate, region E, Fig. 4, and will be below the temperature of the surrounding plate. The sensor itself can have internal structure that would limit conduction to its center and further lower the temperature of the sensor body. Evaluation of the present configuration with liquid crystals showed that the center of a test sensor was several degrees below the temperature of the surrounding region E.

A sensor that is at a lower temperature results in a smaller surface to flow temperature difference and thus a reduced heat flux actually leaving the sensor. However, if the temperature of the sensor is known a correction can be estimated. The temperature of the sensor can be found directly if a temperature sensor is included in the sensor body. This is the simplest solution. If no temperature sensor is available, liquid crystals on and around the sensor surface can give an estimate of the temperature distribution. However, liquid crystals are not simple to use and there is likely a change in surface radiative properties and perhaps some flow disturbance due to their presence. Planned changes to the heated plate will allow direct heating of the sensor housing.

Uncertainty on the sensor temperature translates to uncertainty on the sensor heat flux value. This translation is not simple in that a non-uniform temperature profile in the sensor region will change the thermal boundary layer profile. However, computational results have shown that the boundary layer in the present test section recovers

quickly relative to the sensor dimensions and that the error in assuming an undisturbed heat transfer coefficient profile will be small relative to other uncertainties [10].

B. *Sensor radiation heat flux*

The sensor analysis is very similar to that for the reference area, except that the emissivity of test sensors will vary and will typically be near unity. A typical sensor may have $\varepsilon_{sensor} = 0.85$ with some manufacturer supplied uncertainty on this value. Assuming the sensor sees only room temperature black surroundings, the radiative flux from the sensor will be $q''_{rad,sensor} = 247$ W/m^2 at $\Delta T_{flow} = 40$ K, or 9.2 % of the total flux from the sensor. Uncertainty in ε_{sensor} will strongly affect $q''_{rad,sensor}$ which will in turn affect the uncertainty on q''_{total}. To control the total uncertainty due to this radiation component, the emissivity of the sensor surface must be supplied by the manufacturer. Heating of the test section upper surface would largely eliminate this uncertainty and is being planned for the second generation design.

III. Computational Modeling

A. *Flow/ plate conjugate solution*

The solution to the test section conjugate (coupled conduction/convection) heat transfer problem is required to know the heat flux distribution in the flow direction along the plate. The heat flux distribution is required to translate the reference heat flux averaged over the reference area to the sensor heat flux value averaged over the smaller sensor surface. These values differ due to the non-linear heat flux distribution.

A computational model of the flow and plate has been developed at NIST [10]. It is a two-dimensional solution of the full thermally-compressible Navier-Stokes equations including buoyancy and transient effects. The code models thermal conduction within the plate and insulation, and convection and diffusion in the laminar boundary layer above the plate. The code has predicted heat flux with original plate and insulation design, using nozzle exit velocity measurements, Fig. 3, as input. The predicted heat flux along the plate for a 40 K surface to flow temperature difference is shown in Fig. 6. The flux is seen to drop rapidly, coming to a more uniform value across the region of the sensor at 40 mm downstream. The peak in the flux occurs at the leading edge of the plate after a rise across a 3.2 mm layer of balsa wood insulating the heated plate from the aluminum contraction nozzle.

The calculated heat flux profile (Fig. 6) allows comparison of the average flux from the reference area versus the average flux from the sensor. The typical sensor has a small sensing area that can be taken as a point measurement. Using the results of the numerical solution and integrating across the reference area gives a comparison of the average flux over the reference area to the flux at the center which is equivalent to the flux seen by the sensor. This gives $q''_{sensor} / q''_{ref} = 0.969$. This agrees with the theoretical value (based on a distribution of $x^{-1/2}$) found earlier of 0.969 and is the difference between the measured reference flux and that seen by the sensor, assuming $T_{sensor} = T_{ref}$. The accuracy of this 3 % correction is very good based on agreement of theory with the numerical modeling results and with facility measurements (discussed below). The resulting uncertainty is therefore on the order of 0.1 % (0.969 $\pm$ 0.001).

B. *Conduction model*

A simpler non-coupled model of the thermal field in the plate and sensor is under continued development with the intent of investigating issues related to improvement of the present plate design [11]. This model includes the convective flow as a boundary condition on the upper surface of the plate using the $x^{-1/2}$ theoretical heat transfer distribution. This reduces convergence times and is reasonable given that the temperature variation in the plate is much less than the plate to flow temperature difference.

Results from this model have clearly shown the presence of gradients in the plate primarily due to the conduction of energy required to heat the bridge between regions. The thermal contours in the gap region for the present plate are shown in Fig. 7. At the ideal balanced condition, the surface of each region in the plate would be isothermal and all regions would be at the same temperature. In actuality, there are several hundredths of a degree Kelvin temperature variation along the surface near the bridge as well as within the bridge, as seen in Fig. 7. Experimentally, a temperature measurement is made with a small thermocouple bead near the surface of the plate (inserted in a hole from the bottom side). Since the desired accuracy of temperature measurement across the bridge is of the same order as the temperature variation seen due to thermal gradients, it is clear that the choice of materials, bridge design, and placement of thermocouples are important issues in the redesign of the heated plate.

REPEATABILITY TESTS

Two test series are reported. The first series examines the ability of a heater control algorithm to arrive at the same reference heat flux value given a randomized start condition and the same external boundary conditions. The second series examines sensitivity of the reference heat flux value to installation factors including sensor housing, heated plate and insulation, and test section structure.

For both test series, the plate to flow temperature difference was set to 40 K. Power to the plate heaters was shut off between tests and the plate allowed to cool. Tests were begun by allowing the heater control program to turn on the power and bring the plate temperatures to a balanced state. The "balanced" condition requires that the final plate to flow temperature difference equal the set temperature difference (within 1 K for these tests), and that the average differential temperature on each side of the reference region equals zero within some convergence criteria, set to 0.015 K for these tests. After balancing the plate temperatures, all system parameters were automatically saved to file and then the system typically left at this stable condition for several hours to monitor system drift. The reference heat flux values are normalized on the actual temperature difference.

These tests were performed using an improved test section support structure that differs from that reported in [12]. The new arrangement allows more accurate alignment of the plate leading edge and upstream thermal guard to the contracting nozzle exit so that the air flow is passed along a smooth surface into the test section. This is a critical issue due to the thin boundary layer, 0.5 mm thick, at nozzle exit, Fig. 3.

First test series: convergence repeatability

In the first test series, a total of 13 data points were collected over a period of 10 days. These data points are presented in Fig. 8 as a function of time. The test section was left undisturbed throughout the series. The power to the plate heaters was shut off for a short time (typically 20 min) between tests and a random array of power settings (within 20% of the final converged power levels) was sent to the plate heaters at the start of each test. The control algorithm then balanced the plate temperatures and saved data to file after the plate had "converged" as defined in the software. The first-order exponential time constant for the plate was 7 minutes. The average time required to reach convergence was approximately 6 hours.

After the first 10 data points were taken (in the course of a week) it appeared that there was an exponential rise in the data to some more stable value after the first three or four data points. This would indicate a much longer system time constant in operation, perhaps due to very slow heating of the support structure around the test section and thermal expansion effects. To check this, the test section was allowed to cool for three days and then the final three data points taken. They appear to confirm the rise seen in the first three data points. The variation seen in points 4 through 10 may be more representative of the lateral conduction uncertainty with the current control algorithm, while the exponential rise is likely an indicator of a real change in the reference flux due to changes in the convective boundary layer, rather than reference heat flux measurement error.

Using all these data gives a sample mean of $q''_{ref,avg} = 2647$ W/m^2 and sample standard deviation of $s = 17$. The tail area probability at the 0.025 level of the t distribution with 12 degrees of freedom is $t_{12,0.025} = 2.179$. This gives a 95 % level of confidence on the true mean of $q''_{ref} = q''_{ref,avg} \pm s \cdot t_{12,0.025} = 2647 \pm 38$ ($\pm$ 1.4 %). This value indicates the accuracy of the control algorithm and also stability of the facility over 10 days time with heating and cooling of the plate and support structure. If points 4 through 10 are isolated to remove the long term transient, then the 95 % level of confidence on the true mean is $q''_{ref} = q''_{ref,avg} \pm s \cdot t_{6,0.025} = 2661 \pm 21$ ($\pm$ 0.8 %). This value indicates repeatability assuming the facility has been in operation for several days. It is likely that this long time constant effect is mostly correctable and that this lower repeatability estimate is achievable. This U = 0.8 % measured (type A) expanded uncertainty of the reference heat flux value gives an indication of the actual lateral conduction uncertainty, but does not include radiation uncertainty. The following test series investigates the added uncertainty of installation variables.

Second test series: installation effects

For the second test series, the sensitivity of the reference heat flux to several installation variables was investigated. Sensitivities of the reference heat flux to re-installation of the sensor, sensor housing, plate position, and test section side walls with upstream thermal guard were investigated. These are not independent variables because the test section side walls cannot be removed without disturbing other parameters, and the plate cannot be removed without disturbing the sensor housing. For some tests, only the sensor housing was removed and replaced. For others, the heated plate was removed and replaced, and several times during the series the entire test section was taken apart and then re-assembled. Each test was begun using the same initial power. However, because the system

was disturbed between each test, the control algorithm was run to bring the system to a balanced condition and then data were written to file.

The converged reference heat flux values are shown in Fig. 9 as a function of time. The mean heat transfer is significantly lower than test series I. After series I was completed, some previous damage to one corner of the test plate was found and repaired resulting in proper alignment of the plate for series II. Therefore, the difference in heat flux is real and due to aerodynamic changes, and the plate positioning for the second test series is in agreement with the computational modeling performed. Figure 9 shows a rise in mean heat flux after the first three points similar to that seen in series I. This also corresponds to the disassembly of the test section side walls and upstream thermal guard after tests 3, 5, and 8. There appears to be some correlation with this action, but the reference heat flux appeared insensitive to all other factors. It was noticed that the thermal guard seemed to change position such that the alignment of the plate to thermal guard and guard to nozzle exit changed during the testing with correlation to the initial rise seen here. Misalignments of approximately 0.1 mm maximum where noted, apparently due to thermal expansion effects. This is a correctable effect and may also explain the rise seen in the first series.

Using these data gives a sample mean of $q''_{ref,avg} = 2331$ W/m^2 and sample standard deviation of $s = 15$. The 95 % level of confidence on the true mean is $q''_{ref} = q''_{ref,avg} \pm s \cdot t_{10,0.025} = 2331 \pm 34$ (± 1.5 %). This precision is in agreement with the series I results. It appears, as desired, that the converged reference heat flux value is insensitive to initial heater power settings, while the variation seen in both series is due primarily to the accuracy of the differential temperature measurement as well as the noted initial transient rise.

CONDUCTION CALIBRATION PLATE TESTS

To further substantiate the accuracy of the facility, a secondary reference has been employed. The conduction calibration plate is a water cooled aluminum plate with a mirror finish that sits above the heated plate separated by precision ball bearings (mounted in a rubber gasket) at its edges. Stagnant room air is the conducting gas with known thermal conductivity [13]. This provides a reference conduction heat flux based on a known temperature difference across an air gap with a known separation distance. The mirror finish minimizes radiation heat transfer, and the surface hemispherical spectral reflectance of the cold plate has been measured (the total hemispherical emissivity, integrating over the IR spectrum, is $\varepsilon = 0.020$) so that radiation can be accurately accounted for. Radiation and conduction combined give a total flux that serves as a secondary absolute reference which can be compared to the measured system reference heat flux.

Uncertainty analysis of calibration plate heat flux

The reference flux of the conduction calibration plate will be called the predicted value, q''_{pred}. Sources of uncertainty in this value are listed in Table 1. All uncertainty estimates are type B (based on information other than statistical analysis of sampled data). Following Table 1: the estimate for the uncertainty on k_{air} (1 %) is given by the authors of the NIST Air Properties Database [13] as generally applicable to gas phase thermal conductivity measurements. A careful study of the effects of humidity on thermal conductivity, based on the work of Melling et. al. [14], showed that for typical mole fractions of water in room temperature air, humidity variation has only a small effect on thermal conductivity. The uncertainty on the separation between the plates is due to plate flatness considerations. Temperature uncertainty refers to the uncertainty on the temperature difference between the two plates. The effect on the reference heat flux of the uncertainty of the emissivity values for the hot and cold plates was determined by perturbing their values in the q''_{pred} calculation. The infinite plate uncertainty is an estimate for this configuration of the uncertainty associated with assuming infinite parallel plate radiation exchange between finite plates.

Clearly, the uncertainties on the thermal conductivity and gap height are the largest uncertainties, with a combined relative standard uncertainty of $u_c = 1.3$ %. Assuming the measured calibration plate reference heat flux values, q''_{pred}, follow a normal distribution, with a standard deviation of approximately 1.3 %, the actual true heat flux will be $q''_{pred,avg} \pm 2.6$ %, where $U = 2.6$ % is the expanded uncertainty and a coverage factor of $k = 2$ has been applied so that the unknown true value lies within the interval of $U = k \cdot u_c$ with a level of confidence of approximately 95 %.

Calibration plate results

The results of 11 tests over a one week period are presented in Table 2. Tests were performed at a nominal temperature difference, $T_{hotplate} - T_{coldplate} = 80$ K, with a separation distance of 3.18 mm. The system was disturbed between each test, requiring re-balancing of the power to the heaters. Before each test the surface of the mirror was

cleaned (outgassing of the gasket caused some organic condensate to collect near the cold plate edges), and the cold plate reset above the hot plate. Between several tests the sensor housing was removed and replaced. In Table 1, q''_{ref} is the converged flux of the heated plate reference section. The reference flux of the conduction calibration plate, q''_{pred}, is the calculated flux for the hot and cold plate temperatures for each test. The normalized value adjusts each q''_{ref} to the average $q''_{pred,avg}$. The reason for the higher q''_{ref} for the first and last tests is not clear.

These data give a sample mean of $q''_{ref,avg} = 750.2$ W/m^2 and sample standard deviation of $s = 2.3$ W/m^2. The tail area probability at the 0.025 level of the t distribution with 10 degrees of freedom is $t_{10,0.025} = 2.228$. This gives a 95 % level of confidence on the true mean of $q''_{ref} = q''_{ref,avg} \pm s \cdot t_{10,0.025} = 750.2 \pm 5.2$ ($\pm$ 0.7 %). These tests demonstrate the excellent repeatability of the heated plate reference section, better than found in the convection repeatability tests (0.7 % vs. 1.5 % uncertainty). The increase of uncertainty in the presence of convection is due at least in part to the added uncertainty associated with an aerodynamic boundary layer and non-uniform heat flux.

The most important result of these tests is demonstration of the heated plate reference section accuracy. In this case, the heated plate reference heat flux, $q''_{ref,avg} = 750.2$ W/m^2, is 3.3 % above the predicted "true" heat flux value for these tests, $q''_{pred,avg} = 726.5$ W/m^2 (itself with a relative expanded uncertainty of 2.6 %). This 3.3 % error says that at this flux level (730 W/m^2) the lateral conduction losses at the heated plate "balanced" condition amount to 3.3 % of the total flux leaving the top of the heated plate, or 24 W/m^2. At the higher convective flux of 2400 W/m^2 (for $\Delta T_{flow} = 40$ K) this parasitic loss would be unchanged and result in only a 1.0 % error. Therefore, the conduction calibration plate has established the absolute accuracy of the heated plate reference independent of other measures.

FUTURE WORK

Several projects are under way, including evaluation of different heat flux sensors with the present heated plate as well as construction of a second generation heated plate. Interaction with U.S. heat flux sensor manufacturers has led to the acquisition of several common types of sensors that will be tested in the convection facility. Testing of these sensors will lead to better understanding of performance in convective versus radiative environments.

The second generation heated plate is being designed to reduce system uncertainty on the reference heat flux, to allow multiple sensor locations and redundant references, and to reduce uncertainties on the flux through the sensor. The conduction code discussed earlier has been used to investigate different reference section designs. Uncertainty on lateral conduction is being reduced with a gap redesign and an increase in the number of independently heated plate regions. Sensor flux uncertainties will be reduced through more direct heating of the sensor and also through use of a heated test section upper surface to control radiation losses. The goal is to reduce relative expanded uncertainty on the reference heat flux to below the 2 % level.

CONCLUSIONS

The NIST convective heat flux calibration facility has seen continued development to its present state as a fully operational facility allowing automated balancing of plate temperatures and measurements of reference heat flux with a repeatability of $\pm$ 1.5 %. An uncertainty analysis on the reference region heat flux value has shown lateral conduction to surrounding regions of the plate to be the greatest source of uncertainty with plate surface emissivity the only other significant source. The calculated relative expanded uncertainty (95 % level of confidence) on the measured reference heat flux value is $\pm$ 4.6 %. Accuracy of the measured reference heat flux value has been judged by comparison to theory, numerical modeling, and independent conduction calibration plate results. The repeatability test series II average heat flux of 2331 W/m^2 is 1.9 % below the numerical model prediction of 2376 W/m^2 corrected for radiation. This 1.9 % difference between measured and predicted values supports the accuracy of the facility and numerical code. Likewise, the conduction calibration plate results demonstrate that at a flux level of 2400 W/m^2 the measured reference heat flux is 1.0 % above the conduction calibration plate's independent reference flux. This 1.0 % difference gives a direct measure of the absolute accuracy of the convection facility and compares favorably with the calculated 4.6 % uncertainty.

Work continues on design of the second generation heated plate, and test measurements with the current facility configuration.

ACKNOWLEDGMENTS

The support of Prof. Alfonso Ortega (University of Arizona) and of Mr. Kenneth Steckler (NIST Building Fire Research Laboratory) on the wind tunnel design is greatly appreciated. The contributions of Dr. David Blackburn (NIST Electronics and Electrical Engineering Laboratory) and Dr. Ronald Davis with Ms. Elizabeth Moore (NIST Chemical Science and Technology Laboratory) to the numerical modeling have been and will continue to contribute

to this work. Mr. Robert Zarr's (NIST Building Fire Research Laboratory) thermal conductivity measurements are also appreciated. The assistance of Dr. Daniel Friend (NIST Chemical Science and Technology Laboratory) with thermal conductivity issues is much appreciated. The help of Dr. Leonard Hanssen (NIST Physics Laboratory) with hemispherical reflectance measurements is greatly appreciated. Finally we acknowledge the support and guidance of Dr. William Grosshandler (NIST Building Fire Research Laboratory, Fire Science Division, Fire Sensing Group leader).

REFERENCES

[1] Diller, T.E., "Heat Flux Calibration -- Progress Toward National Standards," Proceedings of the 41st International Instrumentation Symposium, Denver, CO, May 7-11, 1995.

[2] Moffat R.J., Danek C., "Final Report: The NIST/NSF Workshop on Heat Flux Transducer Calibration," at NIST in Gaithersburg, MD, January 23 and 24, 1995.

[3] Grosshandler, W.L., Blackburn, D., "Development of a High Conduction Calibration Apparatus," HTD-Vol. 353, Proceedings of the ASME Heat Transfer Division, Vol. 3, pp.153-158, 1997.

[4] Murthy, A.V., Tsai, B.K., Saunders, R.D., "Radiative Calibrations of Heat Flux Sensors at NIST-An Overview," HTD-Vol. 353, Proceedings of the ASME Heat Transfer Division, Vol. 3, pp.159-164, 1997.

[5] Diller, T.E., "Advances in Heat Flux Measurements," Advances in Heat Transfer, v.23, Academic Press, Boston, 1993.

[6] Diller, T. E., "Heat Flux," Ch. 6.3 In The Measurement, Instrumentation and Sensors Handbook, Ed. J. G. Webster, CRC Press, Boca Raton, Florida, 1998.

[7] Keltner, N.R., "Heat Flux Measurements: Theory and Applications," Ch. 8, In K. Azar (ed.), Thermal Measurements in Electronics Cooling, Boca Raton: CRC Press, 273-320, 1997.

[8] Morel, T., "Design of Two-Dimensional Wind Tunnel Contractions," J. Fluids Engineering, pp.371-377, June, 1977.

[9] Wills, J.A.B., "The correction of hot-wire readings for proximity to a solid boundary," J. Fluid Mechanics, v.12, p.388-396, 1962.

[10] Personal communication with R. Davis and E. Moore of NIST Chemical Science and Technology Laboratory.

[11] Personal communication with D. Blackburn of NIST Semiconductor Electronics Division.

[12] Holmberg, D., Steckler, K., Womeldorf, C., Grosshandler, W., "Facility for Calibrating Heat Flux Sensors in a Convective Environment," HTD-Vol. 353, Proceedings of the ASME Heat Transfer Division, V. 3, pp.165-171, 1997.

[13] Lemmon, E.W., "NIST Air Properties Database, SRD #72, Version 1.0," National Institute of Standards and Technology, Gaithersburg, MD, 1998.

[14] Melling, A., et. al., "Interpolation Correlations for Fluid Properties of Humid Air in the Temperature Range 100 °C to 200 °C," J. Physical Chemistry Ref. Data, Vol. 26, No. 4, 1997.

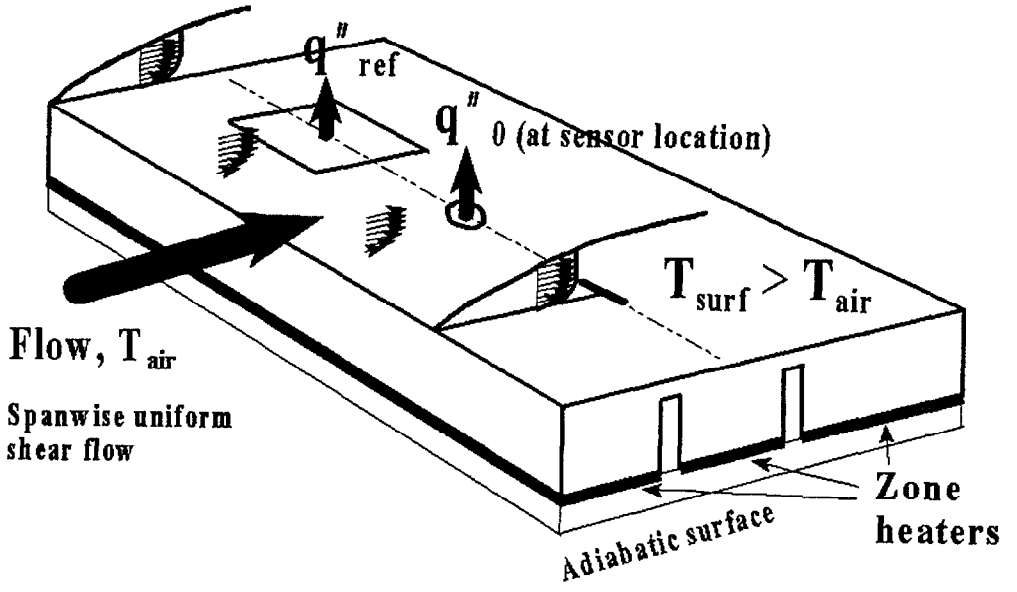

Figure 1: Heated plate below laminar boundary layer with reference region to determine undisturbed heat flux at sensor.

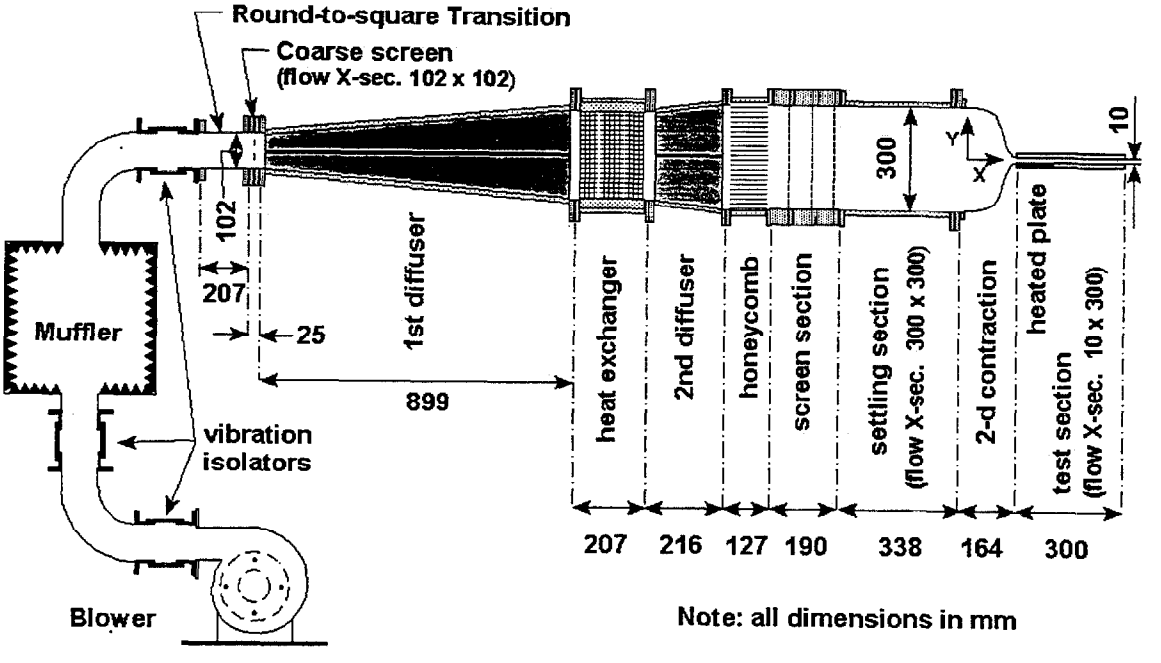

Figure 2: Schematic of wind tunnel and flow conditioning.

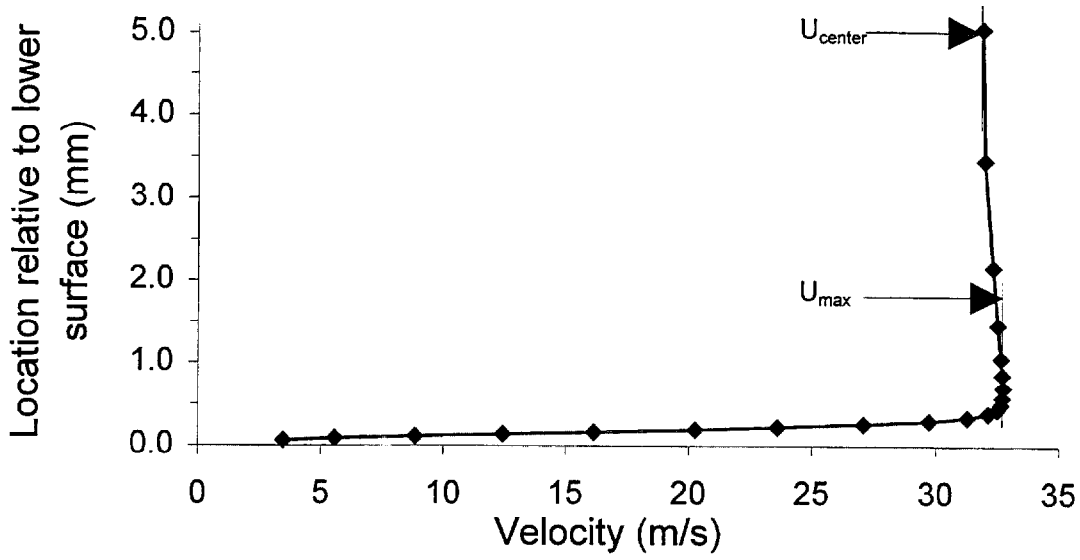

Figure 3: Measured velocity profile of flow exiting lower half of contracting nozzle. Hot-wire data corrected for near-wall effects. The standard uncertainty (estimated standard deviation) is 0.3 m/s except near wall (lower half of boundary layer) where uncertainty rises due to probe/ surface interaction and uncertainty in applied correction.

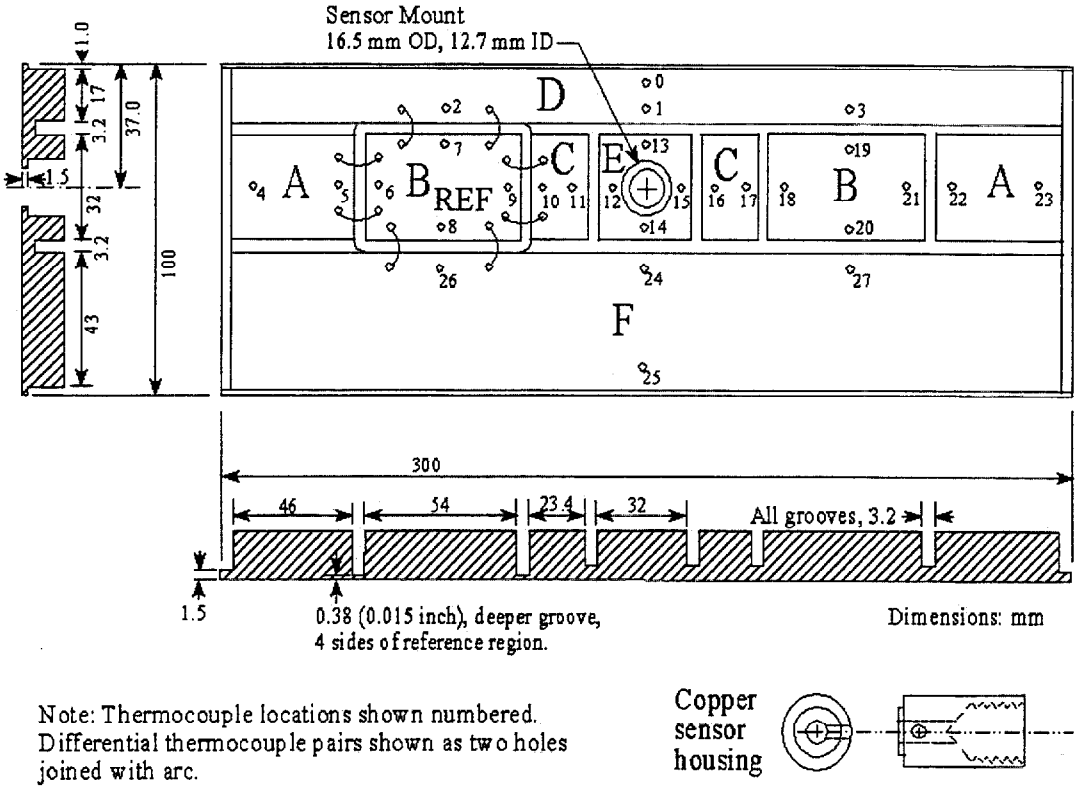

Figure 4: Bottom view of heated plate showing sensor location, separate regions of plate, and sensor holder.

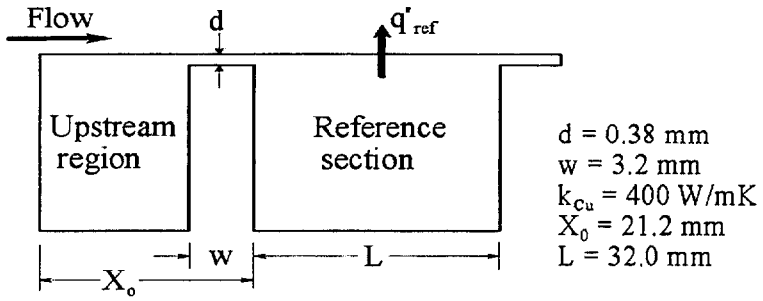

Figure 5: Side view of heated plate reference section and upstream region showing bridge across air gap and dimensions for first generation heated plate.

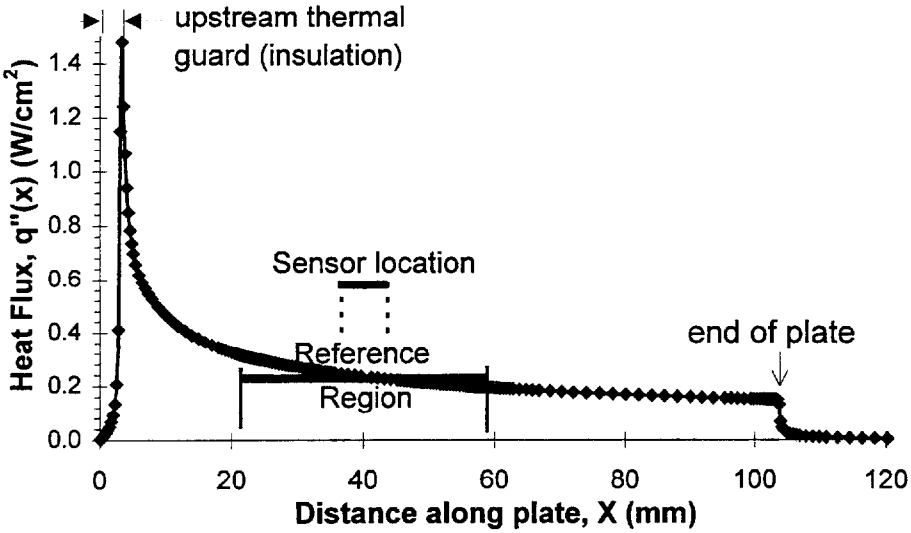

Figure 6: Heat flux along the plate from nozzle exit as predicted by conjugate conduction/ convection numerical model (ΔT_{flow} = 40 K, Re_h = 20,000).

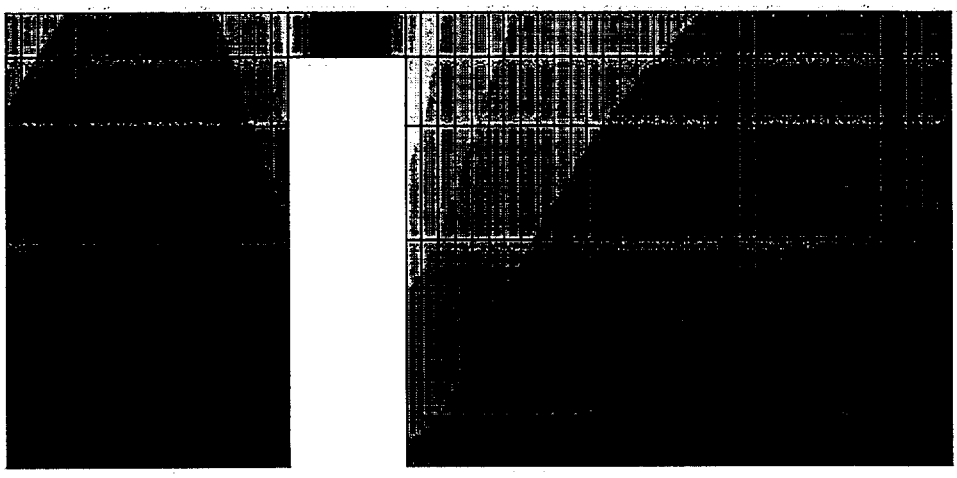

Figure 7: Temperature gradients in plate, looking from side at the upper 2 mm of the plate (same view as in Fig.5), from the center of the upstream region (left) to the center of the reference region (right) for T_{plate} - T_{air} = 40 K, not to scale. Contour gradients, ΔT = 0.01 K.

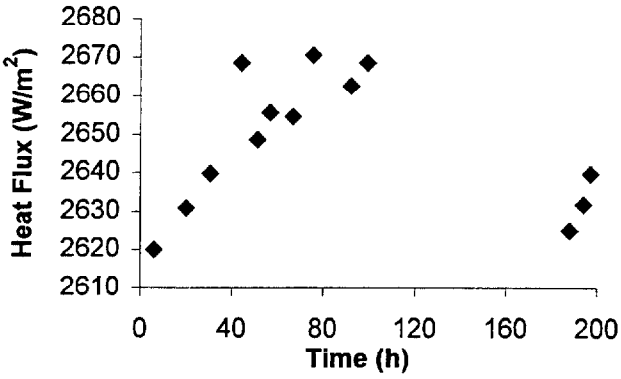

Figure 8: Repeatability test Series I data—converged reference heat flux result of successive measurements with varied initial heater power settings.

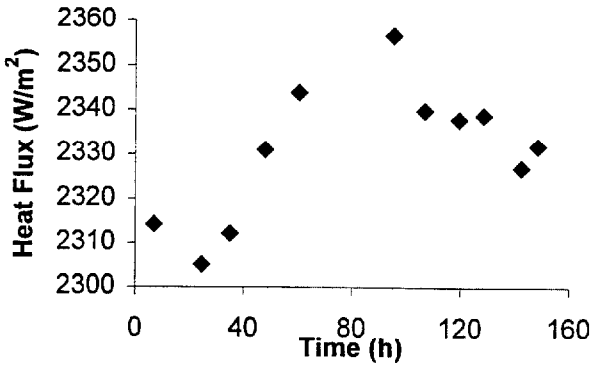

Figure 9: Repeatability test Series II data—converged reference heat flux result of successive runs with varied installation factors.

Table 1 Conduction calibration plate reference heat flux uncertainties.

Uncertainty name	*relative standard uncertainty, u_j (%)*	*source for uncertainty estimate*
k_{air} (thermal cond.)	1.0	ref [12]
humidity variation	0.1	analysis based on ref [13]
h_{gap} (plate sep. distance)	0.8	0.025mm /3.18 mm
temperature difference	0.06	0.05 K/ 80 K
$\varepsilon_{hotplate}$	0.2	perturb 0.03 < $\varepsilon_{hotplate}$ < 1.0
$\varepsilon_{coldplate}$	0.15	perturb 0.015 < $\varepsilon_{coldplate}$ < 0.025
infinite plate assumption	0.1	see expl. In text

Table 2 Results from conduction calibration plate tests.

Test	q''_{ref} (W/m^2)	q''_{pred} (W/m^2)	$q''_{ref,norm}$ $q''_{ref} \times \frac{q''_{pred,avg}}{q''_{pred}}$
1	753.1	725.0	754.7
2	749.4	726.7	749.2
3	750.3	726.6	750.2
4	747.9	726.9	747.5
5	750.8	726.6	750.7
6	749.5	726.8	749.2
7	747.8	727.0	747.3
8	750.3	726.7	750.1
9	748.7	726.7	748.5
10	751.6	726.5	751.6
11	753.3	726.3	753.5
avg	**750.2**	**726.5**	**750.2**
s.d.			**2.3**

NIST-114 (REV. 6-93) ADMAN 4.09

U.S. DEPARTMENT OF COMMERCE
NATIONAL INSTITUTE OF STANDARDS AND TECHNOLOGY

MANUSCRIPT REVIEW AND APPROVAL

(ERB USE ONLY)	
ERB CONTROL NUMBER	DIVISION
PUBLICATIONS REPORT NUMBER: No. NISTIR 6197	CATEGORY CODE
PUBLICATION DATE: December 1998	NO. PRINTED PAGES

INSTRUCTIONS: ATTACH ORIGINAL OF THIS FORM TO ONE (1) COPY OF MANUSCRIPT AND SEND TO: WERB SECRETARY, BUILDING 820, ROOM 125

TITLE AND SUBTITLE (CITE IN FULL)

A PROGRESS REPORT ON THE NIST CONVECTIVE HEAT FLUX CALIBRATION FACILITY

CONTRACT OR GRANT NUMBER

TYPE OF REPORT AND/OR PERIOD COVERED

AUTHOR(S) (LAST NAME, FIRST INITIAL, SECOND INITIAL

D. G. Holmberg, C. A. Womeldorf

PERFORMING ORGANIZATION (CHECK (X) ONE BOX)

- [X] NIST/GAITHERSBURG
- [ ] NIST/BOULDER
- [ ] NIST/JILA

LABORATORY AND DIVISION NAMES (FIRST NIST AUTHOR ONLY)

BFRL, 865

SPONSORING ORGANIZATION NAME AND COMPLETE ADDRESS (STREET, CITY, STATE, ZIP)

PROPOSED FOR NIST PUBLICATION

- [ ] JOURNAL OF RESEARCH (NIST JRES)
- [ ] J. PHYS. & CHEM. REF. DATA (JPCRD)
- [ ] HANDBOOK (NIST HB)
- [ ] SPECIAL PUBLICATION (NIST SP)
- [ ] TECHNICAL NOTE (TN)
- [ ] MONOGRAPH (NIST MN)
- [ ] NATL. STD. REF. DATA SERIES (NIST NSRDS)
- [ ] FEDERAL INFO. PROCESS. STDS. (NIST FIPS)
- [ ] LIST OF PUBLICATIONS (NIST LP)
- [X] INTERAGENCY/INTERNAL REPORT (NISTIR)
- [ ] LETTER CIRCULAR
- [ ] BUILDING SCI. SERIES
- [ ] PRODUCT STANDARDS
- [ ] OTHER
- [ ] —

PROPOSED FOR NON-NIST PUBLICATION (CITE FULLY): [X] —U.S. FOREIGN— [ ]

PUBLISHING MEDIUM:	X	PAPER		DISKETTE		CD-ROM		WWW		OTHER

SUPPLEMENTARY NOTES

ABSTRACT (A 2000-CHARACTER OR LESS FACTUAL SUMMARY OF MOST SIGNIFICANT INFORMATION. IF DOCUMENT INCLUDES A SIGNIFICANT BIBLIOGRAPHY OR LITERATURE SURVEY, CITE IT HERE. SPELL OUT ACRONYMS ON FIRST REFERENCE.) (CONTINUE ON SEPARATE PAGE, IF NECESSARY.)

The National Institute of Standards and Technology has developed a convective heat flux calibration facility to allow evaluation of heat flux sensors. Recognizing that many sensors are used in mixed radiation and convection environments, convective calibrations complement heat flux sensor calibrations presently conducted using standard radiation methods. By extending calibration capabilities to include a primarily convective environment, direct comparisons of sensors in controlled convective and radiative environments are possible.

This report describes the first-generation heated-plate design and performance. An uncertainty analysis of the reference heat flux is presented and repeatability test results are given in support of the uncertainty analysis. Planned tests and development of the second generation heated plate are mentioned.

KEY WORDS (MAXIMUM OF 9; 28 CHARACTERS AND SPACES EACH; SEPARATE WITH SEMICOLONS; ALPHABETIC ORDER; CAPITALIZE ONLY PROPER NAMES)
calibration; convection; heat flux; standards; uncertainty

AVAILABILITY:

- [X] UNLIMITED
- [ ] FOR OFFICIAL DISTRIBUTION - DO NOT RELEASE TO NTIS
- [ ] ORDER FROM SUPERINTENDENT OF DOCUMENTS, U.S. GPO, WASHINGTON, DC 20402
- [X] ORDER FROM NTIS, SPRINGFIELD, VA 22161

NOTE TO AUTHOR(S): IF YOU DO NOT WISH THIS MANUSCRIPT ANNOUNCED BEFORE PUBLICATION, PLEASE CHECK HERE. [ ]